nature chemistry

PERSPECTIVE

PUBLISHED ONLINE: 24 AUGUST 2009 | DOI: 10.1038/NCHEM.327

Charge-shift bonding and its manifestations in chemistry

Sason Shaik[1]*, David Danovich[1], Wei Wu[2]* and Philippe C. Hiberty[3]*

Electron-pair bonding is a central chemical paradigm. Here, we show that alongside the two classical covalent and ionic bond families, there exists a class of charge-shift (CS) bonds wherein the electron-pair fluctuation has the dominant role. Charge-shift bonding shows large covalent–ionic resonance interaction energy, and depleted charge densities, and features typical to repulsive interactions, albeit the bond itself may well be strong. This bonding type is rooted in a mechanism whereby the bond achieves equilibrium defined by the virial ratio. The CS bonding territory involves, for example, homopolar bonds of compact electronegative and/or lone-pair-rich elements, heteropolar bonds of these elements among themselves and with other atoms (for example, the metalloids, such as silicon and germanium), hypercoordinated molecules, and bonds whose covalent components are weakened by exchange-repulsion strain (as in [1.1.1]propellane). Here, we discuss experimental manifestations of CS bonding in chemistry, and outline new directions demonstrating the portability of the new concept.

There are probably only a handful of concepts that are as fundamental and central to chemistry as that of the electron-pair bond. Ever since the ingenious hypothesis of Lewis[1], followed by pioneering work of Heitler and London[2], on the origins of electron-pair bonding, and the colossal intellectual construct of Pauling[3], electron-pair bonding has been traditionally classified into two major families[3–5]. One is the family of covalent and polar-covalent bonds, in which the bonding arises predominantly from stabilization due to the spin-pairing in the covalent structure of the bond. The second family involves the ionic bonds, in which the bonding arises primarily from the electrostatic stabilization of the two oppositely charged fragments. Hence, based on this traditional classification, the bonding type can be characterized by knowledge of the static electronic distribution in the bond, using, for example, electronegativities, or electron-density population analyses provided in standard quantum chemical calculations. However, these traditional classes of bonding cannot describe many intriguing features of bonds, of which we mention two examples, one regarding 'ionic' bonds, the other regarding 'covalent' bonds:

Thus, for example, the bonds $H_3Si^{+0.85}F^{-0.85}$, $Li^{+0.94}F^{-0.94}$ and $Na^{+0.91}Cl^{-0.91}$, where the superscripted number corresponds to group charges, all have 'ionic' charge distribution (determined by charge-density integrations)[5–7]. But, whereas Li^+F^- and Na^+Cl^- behave chemically as genuine ionic bonds, the 'Si^+X^-' bonds (X^- = halide, perchlorate, and other electronegative groups) behave chemically as covalent bonds[8–10].

Another striking example is the difference between H_2 and F_2; two homonuclear bonds that by all criteria should be classified as covalent bonds, but exhibit fundamental differences. Consider the energy curves (Fig. 1) of the two bonds calculated recently[5,11,12]. Figure 1a shows that the H–H bond is indeed covalent; its covalent structure accounts for most of the bonding energy (relative to the 'exact' curve). By contrast, for the F–F bond in Fig. 1b, the covalent structure is entirely repulsive, and what determines the bonding energy and the equilibrium distance is the covalent–ionic mixing. This mixing leads to a resonance energy stabilization, which we have termed the 'charge-shift resonance energy' (RE_{CS}). Thus, despite their apparent similarity, the two bonds are very different; whereas the H–H bond is a true covalent bond, the F–F bond is a CS bond[5,12] that is completely determined by the RE_{CS} quantity. The above-mentioned Si–X bonds are also CS bonds, and the original papers[5,12–14] include a few more puzzling examples that counter the traditional classification. Indeed, our work over the past decade demonstrates that CS bonding constitutes a large and distinct class of bonding alongside the two classical families, and that it possesses unique chemical and physical signatures[5,11–18]. The features of this bond family, its territory and chemical manifestations, are discussed in this Perspective.

Theoretical characterization of bond types

The emergence of three bonding families — covalent, ionic and now CS — was originally derived from modern valence bond (VB) calculations[12]. As expressed in eq. (1), the VB wavefunction (Ψ) of a bond A–X is computed as a combination of the covalent form Φ_{cov} (A•–•X), and two ionic forms, Φ_{ion} (A^+X^-) and Φ'_{ion} (A^-X^+):

$$\Psi(\mathrm{VB}) = c_1\Phi_{cov} + c_2\Phi_{ion} + c_3\Phi'_{ion} \qquad (1)$$

The bond-dissociation energy (D_e) is the energy of this covalent–ionic wavefunction relative to the separate fragments (A• and X•) at their relaxed geometric and electronic structures. Thus, D_e has two contributions; one comes from the bonding energy of the principal VB structure, and the other from RE_{CS} due to the covalent–ionic mixing. The principal VB structure is the one having the lowest energy, and hence also the largest coefficient among the three structures in eq. (1). Its contribution to the bonding energy is referred to as D_{cov} or D_{ion}, wherein the subscript specifies the dominant VB structure. In all cases, RE_{CS} is determined by reference to the principal VB structure, for example, Φ_{cov} in Fig. 1a–d, or Φ_{ion} (Fig. 1e,f).

These quantities characterize the bonding type as can be gleaned from Fig. 1. Thus the principal VB structure for both H–H and B–H is Φ_{cov}, the RE_{CS} quantity is small and much less significant than the large D_{cov} (Fig. 1a,c); in accordance with this, these bonds are

[1]Institute of Chemistry and The Lise Meitner-Minerva Center for Computational Quantum Chemistry, The Hebrew University of Jerusalem, 91904, Jerusalem, Israel. [2]State Key Laboratory of Physical Chemistry of Solid Surfaces and College of Chemistry and Chemical Engineering, Xiamen University, Xiamen 361005, P. R. China. [3]Laboratoire de Chimie Physique, Groupe de Chimie Théorique, CNRS UMR 8000, Université de Paris-Sud, 91405 Orsay Cédex, France. *e-mail: sason@yfaat.ch.huji.ac.il; weiwu@xmu.edu.cn; philippe.hiberty@lcp.u-psud.fr

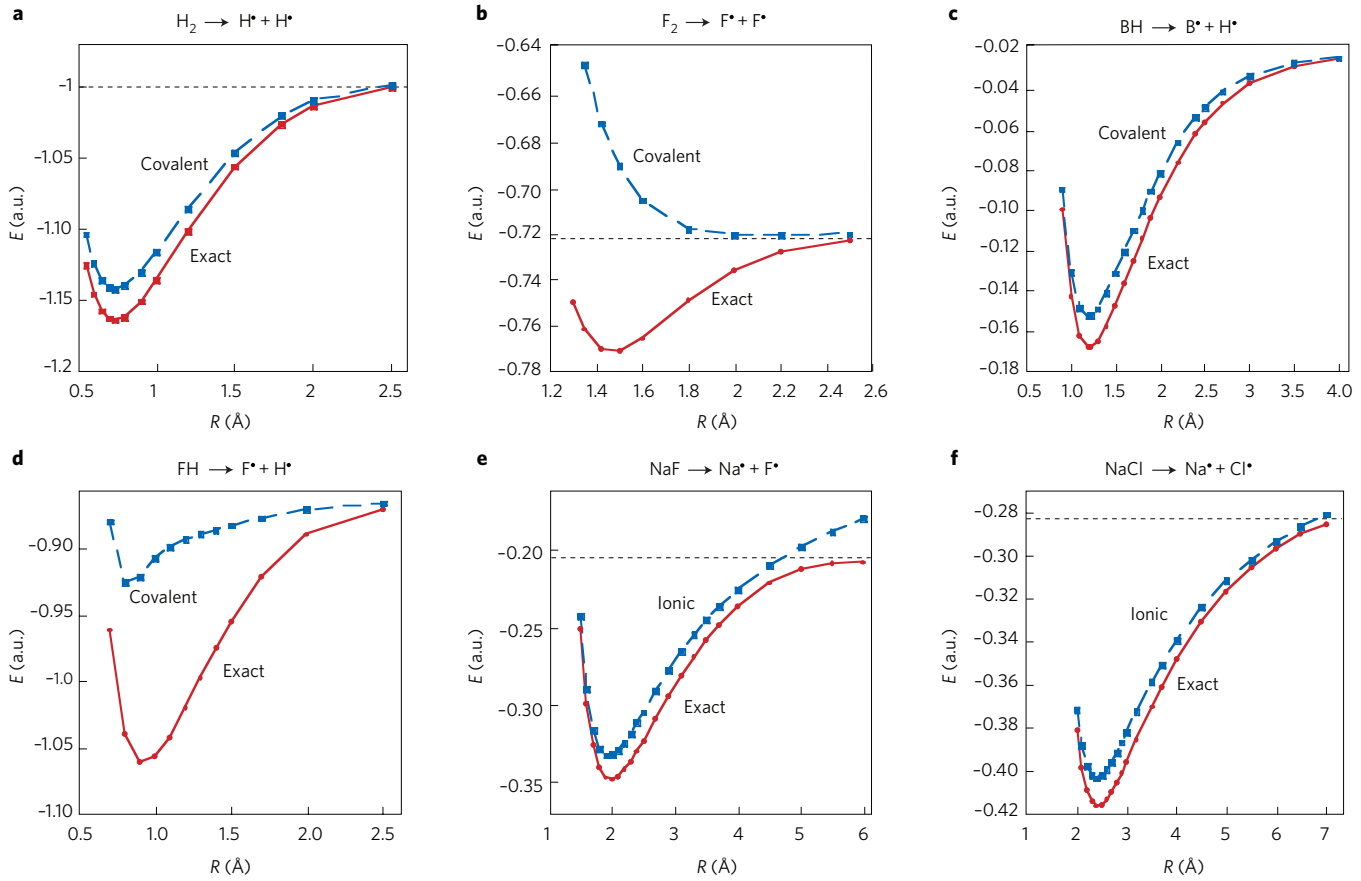

Figure 1 | Valence bond computed energies (*E*) as functions of the interatomic distances (*R*) for some bonds. The principal VB structure is shown in blue and the exact ground state in red; the latter is the covalent–ionic linear combination defined by eq. (1). **a**–**f**, The principal VB structure is the covalent one for H–H (**a**), F–F (**b**), B–H (**c**) and F–H (**d**), and the ionic one for Na–F (**e**) and Na–Cl (**f**). The energy difference between the exact (red) curve and the dominant VB-structure curve (blue), at the minimum distance of the bond, is the charge-shift resonance energy. Parts **a** and **b** are reproduced with permission from ref. 5, © 2005 Wiley.

classical and polar-covalent types, respectively. By contrast, F–H (Fig. 1d) shows a weakly bound principal structure Φ_{cov}, whereas the major contribution to the bond comes from RE_{CS}. An extreme case is the F–F bond (Fig. 1b) in which the principal structure Φ_{cov} is not even bonded, that is, D_{cov} is negative, whereas RE_{CS} is even larger than the total bonding energy. In agreement with this, F–H and F–F are both CS bonds. Finally, in Na–F and Na–Cl (Fig. 1e,f) the principal VB structure is now Φ_{ion}, and the RE_{CS} quantity is a minor contributor, making both classical ionic bonds, where most of the bonding energy arises from the ionic structure.

An alternative way to characterize bonding uses electron-density theories, such as atoms in molecules (AIM)[19] and electron localization function (ELF)[20]. The AIM parameters can be either calculated or derived from density determined experimentally, and are used by experimental chemists to characterize interactions within molecules[21,22]. In this theory, a bond is generally characterized by a bond path, which defines a maximum density path connecting the bonded atoms. The point of the path at which the density is at a minimum is called the bond critical point (BCP), and the values of the density, $\rho(r_c)$, where r_c is the locus of the bond critical point and the Laplacian, $\nabla^2\rho(r_c)$, at this point are characteristic of the bonding type. According to AIM, a classical covalent bond is typified by a significant $\rho(r_c)$ value, and a large negative $\nabla^2\rho(r_c)$. By contrast, closed-shell interactions, which experience Pauli repulsions (also known as overlap repulsion or exchange repulsion), as in ionic bonds, or the He---He interaction, have characteristically a small critical density and a positive Laplacian.

The Laplacian is especially telling[19,23], as it is connected to the kinetic and potential energy densities at BCP, $G(r_c)$ and $V(r_c)$, respectively, by the following local-virial theorem expression:

$$(\hbar^2/4m)\nabla^2\rho(r_c) = 2G(r_c)+V(r_c) \qquad (2)$$

Thus, a negative Laplacian means that the bonding region is dominated by the lowering of the potential energy, whereas a positive Laplacian means that the interaction is typified by excess kinetic energy, and hence is repulsive.

The ELF approach is another topological method, which uses a function related to the Pauli repulsion to carry out a partition of the molecular space into basins of attractors that correspond to the volumes occupied by core inner shells, bonds and lone pairs. As in the Lewis model, a valence basin may either belong to a single atomic shell or be shared by several. In the first case, the basin is called monosynaptic and corresponds to a lone-pair region, and in the second case it is polysynaptic, and specifically bisynaptic for a two-centre bond. The basin population, $\bar{N}$, and its variance, σ^2, are calculated by integrating the one-electron and the pair density over the volumes of the corresponding basins. For a classical covalent bond, the basin is disynaptic, its population is close to 2.0, and the variance is significantly smaller than the population, whereas a classical ionic bond such as NaCl has only core and monosynaptic basins[5,20,24].

To provide a global picture of the various categories of bonds, 27 bonds[5,11–18] are presented in Table 1, and are organized into

three groups, labelled I–III. The first group involves homonuclear bonds from H–H to the 'inverted' C–C bond in [1.1.1]propellane (see Fig. 2c)[18]. Groups II and III involve heteronuclear bonds, from C–H to Si–F. Each bond is characterized by VB properties; the weight of the principal VB structure (ω_{cov}, ω_{ion}), the bonding energy of that structure (D_{cov}, D_{ion}) followed by the full bond-dissociation energy (D_e), and RE_{CS}, followed by the relative resonance energy (%RE_{CS}), which is the percentage ratio of RE_{CS} to D_e. For some of the bonds we show AIM-derived quantities, ρ and $\nabla^2\rho$ as well as the Laplacian components in the BCP for bonding due to the principal structure of the bond ($\nabla^2\rho_{cov}$ or $\nabla^2\rho_{ion}$), and the covalent–ionic resonance ($\nabla^2\rho_{res}$)[11].

Let us first inspect the homonuclear bonds in part I of Table 1, which by all definitions could not possess static bond-ionicities. The bond energies in entries 1–4 are dominated by the covalent component, with RE_{CS} being the minor bonding contribution (<50%). By contrast, the bonds in entries 6–10, all have a bonding energy dominated by RE_{CS} (>100%), whereas the covalent structure is repulsive ($D_{cov} < 0$). The N–N bond, entry 5, is a borderline case, with RE_{CS} accounting for 66.6% of the total bonding energy. Leaving aside the weak Na–Na and Li–Li bonds for which all AIM parameters are close to zero, there is an excellent correlation between the RE_{CS} quantities and the AIM parameters, especially within the same row of the periodic table. Thus, from C–C to F–F (entries 4–7), the resonance component of the Laplacian ($\nabla^2\rho_{res}$) is more and more negative, in agreement with the increase of RE_{CS}, whereas the covalent component ($\nabla^2\rho_{cov}$) goes from negative to positive values, in agreement with the repulsive nature of the covalent structure in CS bonds. As a result, the total Laplacian $\nabla^2\rho$ is large and negative for classically covalent bonds and either a small negative or a positive value for CS bonds. Note that, according to both the RE_{CS} and the experimentally derived $\nabla^2\rho$ values[25], the [1.1.1]propellane molecule embodies the two categories of bonds, classically covalent for the wing bonds (entry 11) and CS bond for the 'inverted' central bond (entry 10).

The same distinction between the covalent and CS bond groups was recently shown to emerge from ELF analysis[5]. Thus, bonds such as H–H, C–C and Li–Li, were found to possess disynaptic basins with a population close to 2.0 and small variances, whereas bonds such as F–F, Cl–Cl, O–O, Br–Br, N–N and the inverted C–C bond of [1.1.1]propellane possess small basin populations[26] (≤1.0), with variances and covariances as large as the population. In the statistical theory of the basin populations, the covariances[5,27] gauge directly the covalent–ionic fluctuations and, usually, are large for the CS bonds and small for the covalent bonds[5]. However, as the covariances show similar trends to the variances we only show the latter in the following discussion. These trends are demonstrated in Fig. 2, which shows the molecular basins for $H_3C–CH_3$, F–F and

Table 1 | A collection of bonds with their VB and AIM properties: group I corresponds to homonuclear covalent and CS bonds, II to heteronuclear covalent and CS bonds, and III to ionic bonds.

I	A–A	ω_{cov}	D_{cov}	D_e	RE_{CS}	%RE_{CS}	ρ	$\nabla^2\rho$	$\nabla^2\rho_{cov}$	$\nabla^2\rho_{res}$
1	H–H	0.76	95.8	105.0	9.2	8.8	0.27	−1.39	−0.70	−0.31
2	Li–Li	0.96	18.2	21.0	2.8	13.1	0.01	−0.01	−0.01	0.00
3	Na–Na	0.96	13.0	13.0	0.0	0.2	0.01	0.00	0.00	0.00
4	$H_3C–CH_3$	0.55	63.9	91.6	27.7	30.2	0.25	−0.62	−0.26	−0.36
5	$H_2N–NH_2$	0.62	22.8	66.6	43.8	65.7	0.29	−0.54	−0.02	−0.68
6	HO–OH	0.64	−7.1	49.8	56.9	114.3	0.26	−0.02	+0.46	−0.75
7	F–F	0.69	−28.4	33.8	62.2	183.9	0.25	+0.58	+1.00	−0.83
8	Cl–Cl	0.64	−9.4	39.3	48.7	124.1	0.14	+0.01	+0.14	−0.26
9	Br–Br*	0.71	−15.3	44.1	59.4	143.8	—	—	—	—
10	C–C_i(prop)†	0.62	−2.2	~70	72.2	>100	0.19‡	+0.43‡	—	—
11	C–C(prop)†	~0.55	—	—	—	—	0.25‡	−0.51‡	—	—
II	**A–X**	ω_{cov}	D_{cov}	D_e	RE_{CS}	%RE_{CS}	ρ	$\nabla^2\rho$	$\nabla^2\rho_{cov}$	$\nabla^2\rho_{res}$
12	$H_3C–H$*	0.69	90.2	105.7	15.1	14.3	—	—	—	—
13	$H_3Si–H$*	0.65	82.5	93.6	11.1	11.9	—	—	—	—
14	B–H	0.71	78.2	89.2	11.0	12.3	0.19	−0.61	−0.59	−0.04
15	Cl–H	0.70	57.1	92.0	34.9	37.9	0.26	−0.81	−0.33	−0.42
16	F–H	0.52	33.2	124.0	90.8	73.2	0.38	−2.52	−1.82	−0.52
17	$H_3C–F$*	0.45	28.3	99.2	70.9	71.5	—	—	—	—
18	$H_3C–Cl$*	0.62	34.0	79.9	45.9	57.4	—	—	—	—
19	$H_3Si–Cl$*	0.57	37.0	102.1	65.1	63.8	—	—	—	—
20	$H_3Ge–Cl$*	0.59	33.9	88.6	54.7	61.7	—	—	—	—
21	F–Cl*	0.59	−39.7	47.9	87.6	182.9	—	—	—	—
22	Cl–Br*	0.69	−9.2	40.0	49.2	123.0	—	—	—	—
III	**A^+X^-**	ω_{ion}	D_{ion}	D_e	RE_{CS}	%RE_{CS}	ρ	$\nabla^2\rho$	$\nabla^2\rho_{ion}$	$\nabla^2\rho_{res}$
23	Li–F	0.76	93.3	104.5	11.2	10.7	0.07	+0.62	+0.51	−0.01
24	Na–F	0.72	77.0	86.0	9.0	10.4	0.05	+0.37	+0.27	+0.02
25	Li–Cl	0.56	76.8	88.5	11.7	13.3	0.04	+0.24	+0.16	0.00
26	Na–Cl	0.63	71.4	79.5	10.1	8.1	0.03	+0.18	+0.13	0.00
27	$H_3Si–F$*	0.36	103.8	140.4	36.6	26.1	—	—	—	—

*From ref. 5. All other data are from ref. 11 unless noted otherwise.
†C–C, (prop) is the inverted bond in [1.1.1]propellane, the other C–C(prop) is one of the wing bonds of the same molecule. The VB data are from ref. 18.
‡Experimental data of Luger *et al.*[25], for a substituted [1.1.1]propellane derivative. The values for the wing bonds are averaged.
Energies are in kcal mol^{-1}, ρ in a.u. (ea_0^{-3}), $\nabla^2\rho$ in a.u. (ea_0^{-5}), where e is the electron charge and a_0 the Bohr radius.

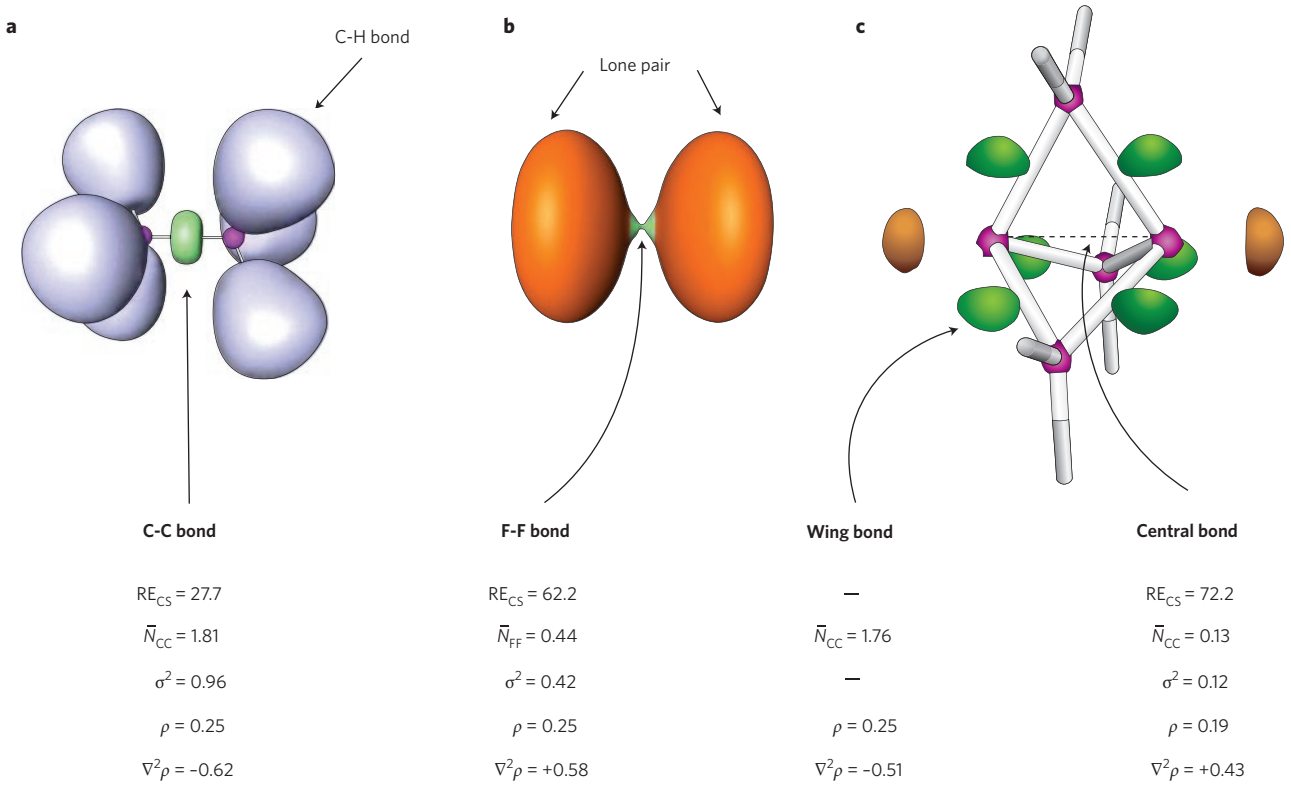

Figure 2 | Some ELF representations of electron density in a few typical cases. **a**, The ELF disynaptic basin[5] for H_3C–CH_3. **b**, The monosynaptic basins[5] for the F–F bond. **c**, Disynaptic basins for the wing bonds of [1.1.1]propellane, and two monosynaptic basins for the central inverted bond[26]. The nature of each bond is further characterized by RE_{CS}, the ELF basin population $\bar{N}$, and its variance σ^2, the density ρ at the bond critical point and the corresponding Laplacian $\nabla^2\rho$ (energies are in kcal mol^{-1}, densities in ea_0^{-3}, Laplacians in ea_0^{-5}).For H_3C–CH_3 and F–F, the ELF and AIM parameters are taken from refs 5 and 11, respectively. For [1.1.1]propellane, the AIM parameters are experimental values[25] (averaged for the wing bonds) from the study of a substituted [1.1.1] propellane derivative. The ELF drawings in **a** and **b** are reproduced with permission from ref. 5, © 2005 Wiley. The ELF drawing in **c** is reproduced with permission from ref. 26, © 2007 Wiley.

C–C in [1.1.1]propellane, alongside their VB and AIM properties. Furthermore, it is seen in Fig. 2b,c that the disynaptic basins of F–F and the inverted C–C bond of propellane are in fact two monosynaptic basins, much like dissociated bonds. Thus, the three methods of diagnosing bonding agree on the classification of homonuclear bonds into two families, and the VB method brings additional energetic insight that highlights the dominant role of the RE_{CS} energy in the CS bond group.

Turning back to heteropolar bonds in part II in Table 1, we note the following trends. Whereas the covalent VB structure is the principal one for all these bonds, the bonds still fall into two distinct groups. Specifically, entries 12–15 belong to the classical polar–covalent bond family based on their $\%RE_{CS}$, which is well below 50%. By contrast, the bonds in entries 16–22 all have weakly bonded covalent structures, and large RE_{CS} exceeding 50% and in some cases >100%. In part III of Table 1 the principal VB structure of all bonds is ionic. The bonding energies in entries 23–26 are all dominated by the electrostatic contribution to bonding (D_{ion}), with small RE_{CS} contributions. These are classical ionic bonds. Finally, the Si–F bond in entry 27 is special: its principal VB structure is ionic; its static ionicity is large, but its RE_{CS} is significant, much larger than that in the classical ionic bonds in III. Valence bond theory predicts[5] that this bond will be very different from ionic bonds. As already alluded to above, the Si–X bonds behave as though they were covalent despite their large ionicity[8]. Here, in II and III, these bonds and their heavier analogues are clearly marked either as CS bonds (Si–Cl, Ge–Cl)[14] or as bonds with a large CS character (Si–F)[5].

The AIM analysis of the heteropolar bonds in II does not distinguish between the covalent and CS bonds, but the Laplacian components in the BCP show that the CS bonds have more pronounced $\nabla^2\rho_{res}$ values[11] compared with the classical covalent bonds, in line with the dominant RE_{CS} quantity. Interestingly, the ELF analysis[5] of these bonds shows better their CS nature; all having depleted disynaptic basins ($\bar{N}$ = 0.86–1.22) with high variances (0.64–0.68), and the case of Si–F is very similar to F–F, with a meagre population (0.27) and a variance (0.24) that is equal to the population. Finally, the AIM analysis of the classical ionic bonds in III (ref. 11) shows the expected characteristics from closed-shell interactions; all have positive Laplacians that are dominated by the ionic component, $\nabla^2\rho_{ion}$. In agreement with this classification of the classical ionic bonds, ELF shows[5] that these bonds only possess monosynaptic basins.

In summary, CS bonding emerges as a distinct class alongside the covalent and ionic bonds. In VB theory[5,11–18], CS bonding is typified by large RE_{CS}, and in ELF, by a depleted basin population with large variance and covariance[5]. In addition, homonuclear CS bonding is characterized in AIM by a small negative or a positive Laplacian of the electron density[11,28]. It should be noted that the characterization of CS bonding by AIM and ELF electron-density analyses is independent of the theoretical method that is used to compute the wavefunction or electron density; for example, molecular orbital bonding theory or density functionals[5,11], showing that the latter methods effectively account for CS bonding, even if not in the explicit way achieved by VB theory. There is of course a relationship between the VB method and molecular orbital or density-functional-theory-based methods of energy partitioning (Kitaura–Morokuma[29], Ziegler–Rauk[30], Baerends–Bickelhaupt[31]). Although these methods do not, as yet, make provisions to characterize CS bonding, they share a few essential features with the VB model: the major one is the Pauli repulsion

that is the origin of the large covalent–ionic resonance energy. In this respect these energy partition methods should see a difference between bonds such as H_2 and F_2 (ref. 32).

Physical origins of CS bonding

The large RE_{CS} quantity of CS bonds is an outcome of the mechanism necessary to establish equilibrium and optimum bonding during bond formation. This mechanism has been analysed before in detail[5,12,33]; here we present a simpler analysis. By comparing the atomic and covalent radii in the periodic table, one finds that generally $r_{ATOM} < r_{cov}$. This means that as atoms (fragments) bind they shrink. The shrinkage causes a steep increase in the kinetic energy of the fragments, which exceeds the lowering of the potential energy due to the diminished size[34–40]. Thus, the shrinkage tips the virial ratio of the kinetic (T) versus potential (V) energies off-equilibrium ($V/T = -2$ at equilibrium). The covalent–ionic resonance is the means whereby the kinetic energy can be reduced to restore the virial ratio[12,34], and this is true in all bonds. The kinetic energy rise due to shrinkage is proportional to the compactness of bonding partners, and therefore, as the fragments in bonding become more electronegative, and hence more compact, the kinetic energy rise due to shrinkage will get steeper. Moreover, when the atoms (fragments) bear lone-pairs, a three-electron repulsion appears between the σ lone-pair of one fragment and the bonding electron of the other. This effect will destabilize the covalent structure, as envisaged originally by Sanderson[41], who termed this as the lone-pair bond-weakening effect (LPBWE); this Pauli repulsion raises the kinetic energy of the bond, and the effect becomes more severe as the number of lone pairs on the atom increases. As electronegative fragments are also lone-pair rich, the combination of atomic shrinkage and LPBWE causes a high excess kinetic energy. In such cases, the resonance energy that will be required to restore the virial ratio becomes necessarily very large, and one finds bonds with weakened covalent structures and large RE_{CS} quantities. Thus, far from being a mere phenomenological model, CS bonding is a fundamental mechanism that is necessary to adjust the kinetic and potential energy to the virial ratio at equilibrium, in response to the Pauli repulsive strain exerted on the bond.

The above relationships are illustrated in Fig. 3; part a shows a plot of the covalent part of the Laplacian against D_{cov} for homonuclear bonds[11]. In the right lower quadrant, where $D_{cov} > 0$ and $\nabla^2\rho_{cov} < 0$, are the bonds with stabilized covalent bonding. The second group, in the upper left quadrant, involves electronegative and lone-pair-rich atoms and 'inverted carbons', which undergo CS bonding. It can be seen that this bonding-type is associated with weakened covalent spin pairing ($D_{cov} < 0$), owing to lone-pair repulsion, which raises the kinetic energy, as seen from the positive sign of $\nabla^2\rho_{cov}$.

Figure 3b shows the RE_{CS} quantities for homonuclear A–A bonds, plotted against the electronegativity (χ_A) of A. It is seen that in each period, RE_{CS} increases as the electronegativty increases. Figure 3c shows a similar plot but now using both homonuclear and heteronuclear bonds[5], and Fig. 3d shows the same trend for π-bonds[15]. It is apparent that the RE_{CS} quantity of the bond generally increases as the average electronegativity of the bond partners increases. Finally, Fig. 3e shows that the resonance component of the Laplacian that gauges the lowering of the kinetic energy by covalent–ionic mixing also correlates with the average electronegativity of the bond[11]. In this respect we note that what determines the RE_{CS} quantity is not the simple orbital overlap, and in fact, the RE_{CS} increases as the overlap becomes smaller[5,12]. For example, the orbital overlap in H_2 is much larger than in F_2, whereas the covalent–ionic resonance energy behaves in the opposite way. This underscores the relationship of

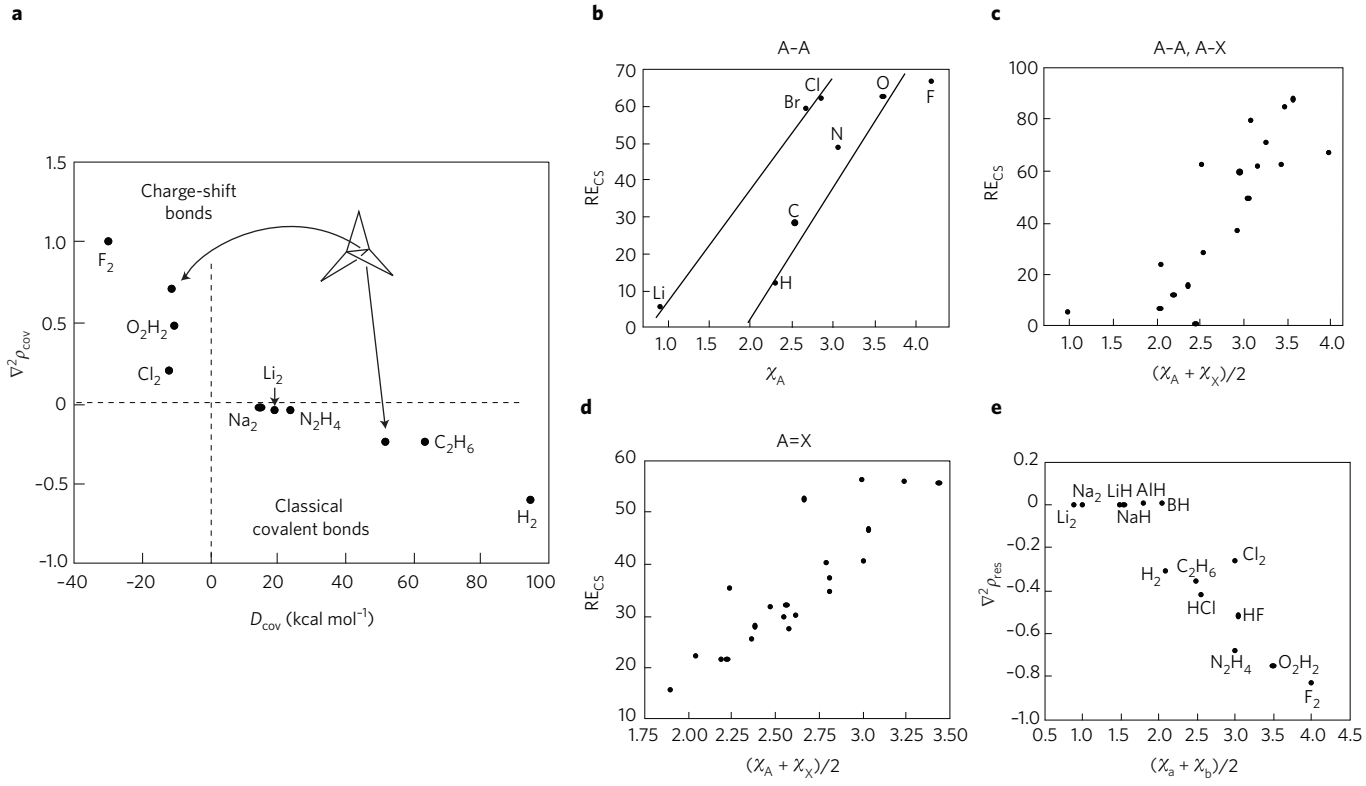

Figure 3 | Correlation of the charge-shift/covalent bond character with the repulsive/attractive nature of the covalent interaction, and with the electronegativities of the bonded atoms. a, The covalent Laplacian, $\nabla^2\rho_{cov}$, versus the covalent bond energy, D_{cov} for a series of homonuclear bonds. **b**, RE_{CS}(A–A) versus the electronegativity of A (χ_A). **c**, RE_{CS} for A–A and A–X bonds versus the average electronegativity of the bond. **d**, RE_{CS} for π-bonds versus the average electronegativity of the bond. **e**, A plot of the resonance Laplacian versus the average electronegativity of the bond. Parts **a** and **e** reproduced with permission from ref. 11, © 2009 Wiley. Parts **b–d** reproduced with permission from ref. 5, © 2005 Wiley.

RE_{CS} to the exchange–repulsion decrease in the bonding region rather than to the simple 'sharing of density' as in covalency.

The exchange–repulsion pressure that is associated with the lone pairs of electronegative fragments is not the only factor that can promote CS bonding. A recently identified additional factor[5,12–14,17] was expressed in bonds between metalloids of group 14 and electronegative groups, for example all the Si–F, Si–Cl and Ge–Cl bonds in Table 1. The VB calculations for these bonds show that the corresponding ionic curve for the Me_3Si–Cl bond, for example, is much deeper than that for the corresponding Me_3C–Cl bond[17]. Moreover, the ionic curve $Me_3Si^+Cl^-$ has a tighter minimum than $Me_3C^+Cl^-$. This means that the Me_3Si^+ ion is smaller than the Me_3C^+ ion along the line of approach to the central atom (silicon or carbon), in harmony with the fact that the charge is completely localized on Si in Me_3Si^+, whereas it is highly delocalized in Me_3C^+. This causes the ionic and covalent structures to be close in energy in Me_3SiCl, thus leading to a high RE_{CS} quantity, which is apparent from Table 1 for the Si–Cl bond[17].

Manifestations of CS bonding

Having shown the emergence of CS bonding and its promoting factors, here we follow with some evidence for the signature of this bond type in the chemical behaviour.

Evidence of CS bonding from electron-density measurements. The existence of the CS bond family will eventually be consolidated by experimental determination of the Laplacian of various bonds, as already done for [1.1.1]propellane derivatives[25], N_2O_4 (ref. 42) and others[21]. In the meantime, the existence of two distinct families already emerges from electron-density-difference maps (measurable experimentally), which plot the difference between the actual molecular density and the density of a reference state made from spherical atoms ($\Delta\rho = \rho_{Mol} - \rho_{Ref}$), at the same geometry as the molecule. These data[43–46] clearly show a bond-group with $\Delta\rho > 0$, which coincides with the classical covalent bond, and a second group of 'no-density bonds' with $\Delta\rho < 0$, which coincides with the CS bonding family. The example of [1.1.1]propellane shows the two bond types[25]; the C–C bonds in the wings are normal covalent bonds with $\Delta\rho > 0$, whereas the 'inverted' (C–C) has $\Delta\rho < 0$. Although the deformation density depends on the definition of the reference atomic state[47], the example of propellanes[43–45], where the same molecule displays two C–C bonds, one having negative and the other positive deformation densities, is free of this limitation.

Evidence for CS bonding in chemical reactivity. The findings that halogen-transfer reactions (and especially of fluorine) have much larger barriers (by >20 kcal mol^{-1} for X = F) than the corresponding hydrogen-transfer processes, is associated with the RE_{CS} quantity of the bond[16]. As we showed recently[16], the barrier difference between the two series follows a very simple relationship:

$$\Delta E^{\ddagger}_{H/XH} - \Delta E^{\ddagger}_{X/HX} = 0.25 RE_{CS} \quad (3)$$

Note that measurement of the barrier difference for the two series enables quantification of the CS resonance energy from experimental barriers.

Rarity of silicenium ions in condensed phases. As Si–X bonds have large RE_{CS} values, their chemical behaviour can be contrasted with carbon, which does not generally involve CS bonds. One of the manifestations is the rare ionic chemistry of silicon in condensed phases[8], compared with the ubiquity in carbon. A recent VB study showed[17] that the $Me_3Si^+Cl^-$ structure in aqueous solution retains the tight ion-pair minimum, and thus mixes strongly with the covalent structure and acquires large RE_{CS}. This large RE_{CS} is the major reason why the bond will not undergo heterolysis in solution (but will prefer associative processes), and why in the solid state even Ph_3Si–$OClO_3$ is a covalent solid[10] by contrast to the carbon analogue, which has an Na^+Cl^--type lattice with Ph_3C^+ and ClO_4^- ions[48] and others[49].

Charting the territory of CS bonding

CS bonding originates from the equilibrium condition of the bond, defined by the virial ratio. It is promoted by two main factors.

First, by exchange repulsion that weakens the covalency of the bond and induces large RE_{CS} values. This excessive exchange repulsion is typical to electronegative and lone-pair-rich atoms, or bonds weakened by exchange–repulsion pressure, as the bridgehead C–C bond in [1.1.1]propellane[18], and many other small-ring propellanes.

Second, fragments that form extremely small cations, which resemble a proton, with all the positive charge located at the central atom, like in the silicenium cation, R_3Si^+, will promote CS bonding especially with electronegative and lone-pair-rich atoms[5,14,17].

With these promoters, CS bonding forms a distinct group of bonding that transcends consideration of static charge distribution, and that possesses unique chemical signatures. Some of these bonds are collected in Table 1. But there are others, for example, π-bonds, in doubly and triply bonded molecules[15,50], and in many hypercoordinated compounds (for example, PCl_5, XeF_n and so on)[5]. Clearly many more CS bonds are waiting to be identified in new molecules.

Future directions are many. A fruitful one is hypercoordination and aggregation. Thus, for example, the small size of R_3Si^+, and heavier analogues, mean that they will tend to form hypercoordinated compounds; in solution, in the solid state[51] and even in the gas phase, where some unusual molecules have been reported[52,53], and bridged $(Si{---}X{---}Si)^+$ systems, which participate in catalytic bond exchange reactions[54]. Metal–metal bonds in some bimetallic complexes could well be CS bonds, as in $M_2(formamidinate)_4$ complexes (M = Nb, Mo, Tc, Ru, Rh, Pd) where large positive values of $\nabla^2\rho(r_c)$ have been reported[55]. Other directions involve the generation of [1.1.1]propellane in which the CH_2 wings are substituted by heteroatoms that exert exchange repulsion pressure on the inverted C–C bond, for example, HN, O and S (ref. 18). The in-plane π-type bond in *ortho*-benzyne is another bond that is affected by exchange–repulsion pressure. Protonation or methylation (by Me^+) of C–N bonds may convert them into CS bonds[56], a fact that may concern DNA bases, and may have mechanistic effects, as in the protonated arginine in the mechanism of nitric oxide synthase[57]. Most bonds under immense external pressure[58] are likely to be CS bonds, and encapsulated highly positive ions will be CS-bound[59,60].

Thus, CS bonding is not merely an academic abstraction. As new examples or experimental manifestations of CS bonding will start to accumulate and be recognized, the concept of CS bonding will gradually be accepted by the chemical community, and will find more applications.

References

1. Lewis, G. N. The atom and the molecule. *J. Am. Chem. Soc.* **38,** 762–785 (1916).
2. Heitler, W. & London, F. Wechselwirkung neutraler atome un homöopolare bindung nach der quantenmechanik. *Zeits. für Physik.* **44,** 455–472 (1927).
3. Pauling, L. *The Nature of the Chemical Bond* (Cornell Univ. Press, 1939).
4. London, F. Zur quantentheorie der homöopolaren valenzzahlen. *Zeits. für Physik A* **46,** 455–477 (1928).
5. Shaik, S., Danovich, D., Silvi, B., Lauvergnat, D. & Hiberty, P. C. Charge-shift bonding – a class of electron-pair bonds that emerges from valence bond theory and is supported by the electron localization function approach. *Chem. Eur. J.* **11,** 6358–6371 (2005).
6. Bader, R. F. W. & Nguyen-Dang, T. T. Quantum theory of atoms in molecules–Dalton revisited. *Adv. Quant. Chem.* **14,** 63–124 (1981).
7. Henn, J., Ilge, D., Leusser, D., Stalke, D. & Engles, D. On the accuracy of theoretically and experimentally determined electron densities of polar bonds. *J. Phys. Chem. A* **108,** 9442–9452 (2004).
8. Apeloig, Y. in *The Chemistry of Organic Silicon Compounds* Vol. 1 (eds Apeloig, Y. & Rappoport, Z.) Ch. 2 (Wiley, 1989).

9. Apeloig, Y. & Stanger, A. The first demonstration of solvolytic generation of a simple silicenium ion (R_3Si^+). Access via 1,2-methyl migration. *J. Am. Chem. Soc.* **109,** 272–273 (1987).
10. Prakash, G. K. S. *et al.* Triphenylsilyl perchlorate revisited: ^{29}Si and ^{35}Cl NMR spectroscopy and X-ray crystallography showing covalent nature in both solution and the solid state. Difficulties in observing long-lived silyl cations in the condensed state. *J. Am. Chem. Soc.* **109,** 5123–5126 (1987).
11. Zhang, L., Ying, F., Wu, W., Hiberty, P. C. & Shaik, S. Topology of electron charge density for chemical bonds from valence bond theory: a probe of bonding types. *Chem. Eur. J.* **15,** 2979–2989 (2009).
12. Shaik, S., Maitre, P., Sini, G. & Hiberty, P. C. The charge-shift bonding concept. Electron-pair bonds with very large ionic-covalent resonance energies. *J. Am. Chem. Soc.* **114,** 7861–7866 (1992).
13. Lauvergnat, D., Hiberty, P. C., Danovich, D. & Shaik, S. Comparison of C-Cl and Si-Cl bonds. A valence bond study. *J. Phys. Chem.* **100,** 5715–5720 (1996).
14. Shurki, A., Hiberty, P. C. & Shaik, S. Charge-shift bonding in group IVB halides: a valence bond study of MH_3-Cl (M = C, Si, Ge, Sn, Pb) molecules. *J. Am. Chem. Soc.* **121,** 822–834 (1999).
15. Galbraith, J. M., Blank, E., Shaik, S. & Hiberty, P. C. π-bonding in second and third row molecules: testing the strength of Linus's blanket. *Chem. Eur. J.* **6,** 2425–2434 (2000).
16. Hiberty, P. C., Megret, C., Song, L., Wu, W. & Shaik, S. Barriers of hydrogen abstraction vs halogen exchange: an experimental manifestation of charge-shift bonding. *J. Am. Chem. Soc.* **128,** 2836–2843 (2006).
17. Su, P., Song, L., Wu, W., Shaik, S. & Hiberty, P. C. Heterolytic bond dissociation in water: why is it so easy for C_4H_9Cl but not for C_3H_9SiCl? *J. Phys. Chem. A* **112,** 2988–2997 (2008).
18. Wu, W., Gu, J., Song, J., Shaik, S. & Hiberty, P. C. The inverted bond in [1.1.1] propellane is a charge-shift bond. *Angew. Chem. Int. Ed.* **48,** 1407–1410 (2009).
19. Bader, R. F. W. *Atoms in Molecules: A Quantum Theory* (Oxford Univ. Press, 1990).
20. Silvi, B. & Savin, A. Classification of chemical bonds based on topological analysis of electron localization functions. *Nature* **371,** 683–686 (1994).
21. Coppens, P. Charge densities come of age. *Angew. Chem. Int. Ed.* **44,** 6810–6811 (2005).
22. Coppens, P. *X-ray Densities and Chemical Bonding* (Oxford Univ. Press, 1997).
23. Kraka, E. & Cremer, D. in *Theoretical Models of Chemical Bonding* Part 2 (ed. Maksić, Z. B.) 457–543 (Springer, 1990).
24. Silvi, B. The spin-pair compositions as local indicators of the nature of the bonding. *J. Phys. Chem. A* **107,** 3081–3085 (2003).
25. Messershmidt, M. *et al.* Electron density and bonding at inverted carbon atoms: an experimental study of a [1.1.1]propellane derivative. *Angew. Chem. Int. Ed.* **44,** 3925–3928 (2005).
26. Polo, V., Andres, J. & Silvi, B. New insight on the bridge carbon-carbon bond in propellanes: a theoretical study based on the analysis of the electron localization function. *J. Comput. Chem.* **28,** 857–864 (2007).
27. Lusar, R., Beltrán, A., Andrés, J., Noury, S. & Silvi, B. Topological analysis of electron density in depleted homopolar chemical bonds. *J. Comput. Chem.* **20,** 1517–1526 (1999).
28. Rincon, L. & Almeida, R. On the topology of the electron charge density at the bond critical point of the electron-pair bond. *J. Phys. Chem. A* **102,** 9244–9254 (1998).
29. Kitaura, K. & Morokuma, K. A new energy decomposition scheme for molecular interactions within the Hartree-Fock approximation. *Int. J. Quantum Chem.* **10,** 325–340 (1976).
30. Ziegler, T. & Rauk, A. On the calculation of bonding energies by the Hartree-Fock-Slater method. *Theor. Chim. Acta* **46,** 1–10 (1977).
31. Velde, G. T. *et al.* Chemistry with ADF. *J. Comput. Chem.* **22,** 931–967 (2001).
32. Krapp, A., Bickelhaupt, F. M. & Frenking, G. Orbital overlap and chemical bonding. *Chem. Eur. J.* **12,** 9196–9216 (2006).
33. Hiberty, P. C., Ramozzi, R., Song, L., Wu, W. & Shaik. S. The physical origin of large covalent-ionic resonance energies in some two-electron bonds. *Faraday Discuss.* **135,** 261–272 (2006).
34. Kutzelnigg, W. in *Theoretical Models of Chemical Bonding* Part 2 (ed. Maksić, Z. B.) 1–44 (Springer, 1990).
35. Ruedenberg, K. The physical nature of the chemical bond. *Rev. Mod. Phys.* **34,** 326–376 (1962).
36. Feinberg, M. J. & Ruedenberg, K. Paradoxical role of the kinetic-energy operator in the formation of the covalent bond. *J. Chem. Phys.* **54,** 1495–1591 (1971).
37. Wilson, C. Q. & Goddard, W. A. III. The role of kinetic energy in chemical binding. *Theor. Chim. Acta.* **26,** 195–210 (1972).
38. Rozendaal, A. & Baerends, E. J. A momentum-space view of the chemical bond. I The first-row homonuclear diatomics. *Chem. Phys.* **95,** 57–91 (1985).
39. Ruedenberg, K. & Schmidt, M. Why does electron sharing lead to covalent bonding? A variational analysis. *J. Comput. Chem.* **28,** 391–410 (2007).
40. Bickelhaupt, F. M. & Baerends, E. J. Kohn-Sham density functional theory: predicting and understanding chemistry. *Rev. Comput. Chem.* **15,** 1–86 (2000).
41. Sanderson, R. T. *Polar Covalence* (Academic Press, 1983).
42. Messerschmidt, M., Wagner, A., Wong, M. W. & Luger, P. Atomic properties of N_2O_4 based on its experimental charge density. *J. Am. Chem. Soc.* **124,** 732–733 (2002).
43. Dunitz, J. D. & Seiler, P. The absence of bonding electron density in certain covalent bonds as revealed by X-ray analysis. *J. Am. Chem. Soc.* **105,** 7056–7058 (1983).
44. Dunitz, J. D., Schweizer, W. B. & Seiler, P. X-ray study of the deformation density in tetrafluoroterephthalodinitrile: weak bonding density in the C-F bond. *Helv. Chem. Acta* **66,** 123–133 (1983).
45. Coppens, P., Yang, Y. W., Blessing, R. H., Cooper, W. F. & Larsen, F. K. The experimental charge distribution in sulfur containing molecules. Analysis of cyclic octasulfur at 300 and 100 K. *J. Am. Chem. Soc.* **99,** 760–766 (1977).
46. Savariault, J.-M. & Lehmann, M. S. Experimental determination of the deformation electron density in hydrogen peroxide by combination of X-ray and neutron diffraction measurements. *J. Am. Chem. Soc.* **102,** 1298–1303 (1980).
47. Ruedenberg, K. & Schwarz, W. H. E. Nonspherical atomic ground state densities and chemical deformation densities from x-ray scattering. *J. Chem. Phys.* **92,** 4956–4969 (1990).
48. Gomes de Mesquita, A. H., MacGillavry C. H. & Eriks, K. The structure of triphenylmethyl perchlorate at 85°C. *Acta Crystallogr.* **18,** 437–443 (1965).
49. Kim, K.-C. *et al.* Crystallographic evidence for a free silylium ion. *Science* **297,** 825–827 (2002).
50. Ploshnik, E. *The Triple Bond – A Valence Bond Theory Point Of View* MSc Thesis, Hebrew Univ. (2005).
51. Kost, D. & Kalikhman, I. Hypercoordinate silicon complexes based on hydrazine ligands. A remarkably flexible molecular system. *Acc. Chem. Res.* **42,** 303–314 (2009).
52. Dávalos, J. Z., Herrero, R., Abboud, J.-L. M., Mó, O. & Yáñez, M. How can carbon be covalently bound to five ligands? The case of $Si_2(CH_3)_7$. *Angew. Chem. Int. Ed.* **46,** 381–385 (2007).
53. Fernández, I., Uggerud, E. & Frenking, G. Stable pentacoordinate carbocations: structure and bonding. *Chem. Eur. J.* **13,** 8620–8626 (2007).
54. Panisch, R., Bolte, M. & Müller, T. Hydrogen and fluorine-bridged disilyl cations and their use in catalytic C-F activation. *J. Am. Chem. Soc.* **128,** 9676–9682 (2006).
55. Llusar, R., Beltran, A., Andrés, J., Fuster, F. & Silvi, B. Topological analysis of multiple metal-metal bonds in dimers of the $M_2(formamidinate)_4$ type with N = Nb, Mo, Tc, Ru, Rh, and Pd. *J. Phys. Chem. A* **105,** 9460–9466 (2001).
56. Shaik, S. in *Molecules in Natural Science and Medicine: An Encomium for Linus Pauling* (eds Maksić, Z. B. & Eckert-Maksić, M.) 253–266 (Ellis Horwood, 1991).
57. Cho, K. B., Carvajal, M. A. & Shaik, S. First half-reaction mechanisms of nitric oxide. The role of proton and oxygen coupled electron transfers in the reaction by quantum mechanical/ molecular mechanical calculations. *J. Phys. Chem. B* **113,** 336–346 (2009).
58. Grochala, W., Hoffmann, R., Feng, J. & Ashcroft, N. W. The chemical imagination at work in very tight places. *Angew. Chem. Int. Ed.* **46,** 3620–3642 (2007).
59. Dognon, J.-P., Clavaguéra C. & Pyykkö, P. A predicted organometallic series following a 32-electron principle: $An@C_{28}$ (An=Th, Pa^+, U^{2+}, Pu^{4+}). *J. Am. Chem. Soc.* **131,** 238–243 (2009).
60. Rupar, P., Staroverov, V. N. & Baines, K. M. A cryptand-encapsulated germanium(II) dication. *Science* **322,** 1360–1363 (2008).